Study on the Encapsulation of the MOEMS Acoustic Sensor Based on F-P Cavity

Bingli Jiang, Kuntao Yang & Zhujun Wan

Wuhan National Laboratory for Optoelectronics, School of Optoelectronic Science and Engineering

Huazhong University of Science and Technology, Wuhan 430074, China

Tel: 86-130-3717-6758   E-mail:pop_ice@sina.com

Jiang'an Wang

Institute of Optoelectronics, School of Electronic Engineering, Naval University of Engineering

Wuhan 430033, China

Tel: 86-27-8344-3973   E-mail:bugles1208@hotmail.com

Abstract

The MOEMS (Optical Micro electro mechanical system) acoustic sensor is the new-generation acoustic sensor technology based on the extrinsic Fabry-Perot cavity (EFPI) integrating the MEMS technology, the micro-photonics, and the acoustic sensor technology, with many advantages such as high sensitivity, anti-electromagnetic field, and anti-radio-frequency interference (RFI). The method and loss of the MOEMS acoustic sensor encapsulation are studied in this article, and the result showed that the insertion loss is most sensitive to the angled mismatching, and the cavity length is accurately positioned by the method of reflection spectrum, which has been tested in the experiment.

Keywords: Fiber-optical acoustic sensor, MOEMS, EFPI, Encapsulation

1. Introduction

MOEMS is also called as MEMS (Optical MEMS), and it is the output combining the MEMS (Micro-electro mechanical system) with the Micro-optical technology, and it is the best micro system with high knowledge concentration, high precision, and high performance at present. The MOEMS acoustic sensor is the new sensor integrating the MOEMS techno0lgoy with the optical fiber technology, the laser technology, and the acoustic sensor technology, with the advantages such as the optical fiber sensor and the MEMS silicon microphone. Because of inborn good electromagnetic immunity, environment adaptability, micro-scale technology, and easy integration, it could be widely applied in many measurements of sound field.

According to different light modulation measures, the MOEMS acoustic sensor could be divided into many types such as the intensity modulation type, the F-P cavity type, the optical fiber interference type, and the FBG type. For the sensor based on the EFPT, the interference cavity is composed by air or other non-optical solid dielectric, and by selecting the F-P cavity materials and controlling the manufacturing parameters, the sensitivity of the measurement could be adjusted, and the crossing sensitivity of some parameters could be eliminated, which has been one of research hotspots. In addition, the F-P encapsulation technology in the MOEMS sensor based on EFPI would directly influence the performance and parameters of the sensor. Therefore, the encapsulation process and the loss characteristics of the MOEMS acoustic sensor based on EFPI will be studied in this article.

2. Analysis of the encapsulation loss characteristics

2.1 Head design of the MOEMS acoustic sensor

The head structure sketch of the MOEMS acoustic sensor is seen in Figure 1, and its basic principle is the light intensity modulation based on EFPI. The head of the sensor is composed by a piece of optical fiber, double-plane G-lens (Grin-lens), MEMS membrane, and capillary glass tube. And the F-P cavity is composed by the collimator end face composed by G-lens and optical fiber and the MEMS membrane. When the acoustic wave acts on the MEMS membrane, the membrane vibration would induce the change of the cavity length of the F-P cavity, and the reflected interference light intensity would change also, and the intensity and frequency of the sound could be computed according to the change of the light intensity.

2.2 Theoretical analysis of the loss characteristics

The light coupling of the single optical-fiber collimator with the MEMS membrane in the encapsulation could be regarded as the light coupling of the collimator composed by the input optical fiber and one GRIN lens with the single-mode optical-fiber collimator composed by the output optical fiber and one GRIN lens, and two lenses are respectively located at the images produced by the reflectors (seen in Figure 1).

If the scattering effect induced by the roughness of the reflection face is not be considered, according to the Gaussian beam coupling analysis and the coordinate transformation, the total loss expression of the single optical-fiber collimator could be obtained based on the axial deviation, the radial deviation, and the angled mismatch, where, ω_{r1} and ω_{r2} are the girded radiuses, λ is the wavelength, Z_0 is the axial mismatch, X_0 is the radial mismatch, and θ is the angled mismatch. And the expression of the insertion loss IL is

$$IL(Z_0, X_0, \theta, \omega_{r1}, \omega_{r2}) = -10 \cdot \lg(\alpha \cdot \exp(\varphi)) \qquad \text{(dB)} \qquad (1)$$

Where,

$$\alpha = \frac{4}{\omega_{r2}^2 \omega^2(Z_0) \cdot (A^2 + B^2)} \qquad (2)$$

$$\varphi = -CX_0 + \frac{A(C^2 - D^2) + 2BCD}{2(A^2 + B^2)} \qquad (3)$$

$$A = \frac{1}{\omega_{r2}^2} + \frac{1}{\omega^2(Z_0)} \qquad (4)$$

$$B = \frac{k}{2R(Z_0)} \qquad (5)$$

$$C = \frac{2X_0}{\omega^2(Z_0)} \qquad (6)$$

$$D = \frac{kX_0}{R(Z_0)} + k \cdot \sin(\theta) \qquad (7)$$

$$k = \frac{2\pi}{\lambda} \qquad (8)$$

$$\omega^2(Z_0) = \omega_{r1}^2 \left(1 + \left(\frac{\lambda Z_0}{\pi \omega_{r1}^2}\right)^2\right) \qquad (9)$$

$$R(Z_0) = Z_0 \left(1 + \left(\frac{\pi \omega_{r1}^2}{\lambda Z_0}\right)^2\right) \qquad (10)$$

2.3 Simulation

The software of Matlab is used to simulate and compute the coupling loss of the collimator, and the when the wavelength is 1310nm, and the girded radiuses of the input collimator and the output collimator are 0.37mm, the relation curves between the insertion loss and various mismatches are seen in Figure 3, Figure 4, and Figure 5.

From above figures, it is obvious that the insertion loss is most sensitive to the angled mismatch, the second and the third respectively are the radial mismatch and the axial mismatch.

3. Encapsulation and test of the MOEMS acoustic sensor

3.1 Confirmation of the cavity length

In the encapsulation, the absolute cavity length of the F-P cavity needs to be confirmed, and it could be obtained by measuring the phase change of the reflection spectrum. The intensity of the emitted light is

$$I_r = \frac{r_1^2 + r_2^2 + 2r_1 r_2 \cos\phi}{1 + r_1^2 r_2^2 + 2r_1 r_2 \cos\phi} I_0 \qquad (11)$$

$$\phi = \frac{4\pi L}{\lambda}$$

(12)

, where, r_1 and r_2 respectively are the reflection rates of the collimator end face and the collimator reflection face, L is the cavity length, and λ is the wavelength. From above formulas, the reflection light spectrum is the quasi-cosine curve, and the curve shape is decided by the length of the F-P cavity, and when the cavity length changes, the curve shape changes with it, so the stable reflection light spectrum could uniquely confirm the length of the F-P cavity.

Supposed that the bandwidth of the emitted wave is in 1.3 μm and 1.32 μm, and the light intensities of different wavelengths are equal, the simulation result of the reflection spectrum curves (when the cavity lengths respectively are 106.765 μm, 106.95 μm, and 107.0925 μm) is seen in Figure 6.

3.2 Encapsulation process

The encapsulation of the MOEMS acoustic sensor based on EFPI needs the spectrograph, the microscope, the 3D adjusting bracket, and the micro-positioner. First, fix the MEMS membrane to one end of the glass fiber tube by the glue, and fix the glass fiber tube with the MEMS membrane on the optical platform horizontally by the clamp, and then insert the collimator into the glass fiber tube, and adjust the membrane and the collimator end fact to the level by the 3D adjusting bracket, and then use the micro-positioner to adjust the distance between two end faces, and whether two end faces are parallel and the distance between two end faces could be confirmed by the spectrograph. After the adjusting is completed, coat the glue and fix the sensor head when the glue is solidified.

3.3 Static pressure test and analysis

Test the static pressure of the encapsulated MOEMS sensor head, and link the optical-fiber with the light source and the photoelectric detection circuit respectively by the coupler. The simulation curve and the practical result are seen in Figure 7.

From the figure, it is obvious that the total effect is good, but the practical measurement result is little less than the simulation result. The cause of the error is that the sensor head uses the single optical-fiber design, and it respectively links with the light source and the detection circuit after the beam split coupling where the attenuation occurs.

4. Conclusions

The encapsulation technology of the MOEMS acoustic sensor based on EFPI is studied in the article, and the radial mismatch, the axial mismatch, and the angled mismatch are analyzed in the encapsulation, and the result shows that insertion loss is most sensitive to the angled mismatch. At the same time, the method of the reflection spectrum is used to accurately confirm the cavity length, and the MOEMS acoustic sensor is encapsulated according to this method, and the ideal test result has been proved.

References

Guo, Zhenwu & Li, Weixiang et al. (2007). Analysis of Loss and Development of Fabry-Perot Optical Fiber Sensor. *Instrument Technique and Sensor.* No.5. P.11-14.

Li M, & Wang M. (2006). Optical MEMS pressure sensor based on Fabry-Perot interferometry. *Optical Society of America.* No.14(4).

Wan, Zhujun. (2002). *Study on the Online Two-Stage Optoisolator and the Optical Passive Combination Device in EDFA.* Wuhan: Master's Thesis of Huazhong University of Science and Technology.

Yang, Guoguang. (2008). *Micro-optics and System.* Hangzhou: Zhejiang University Press. P.1-3.
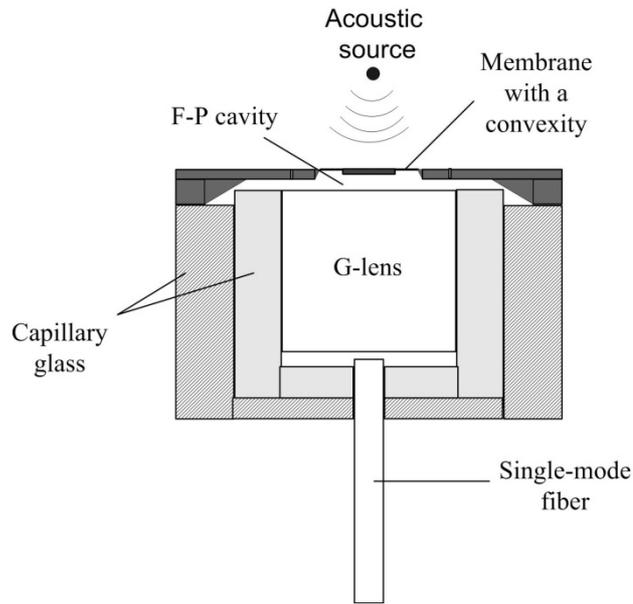
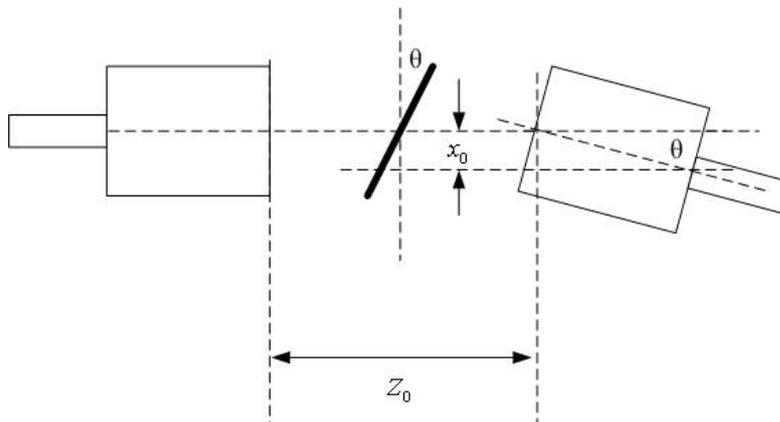Figure 1. Head Sketch of the MOEMS Acoustic Sensor Based on F-P Cavity

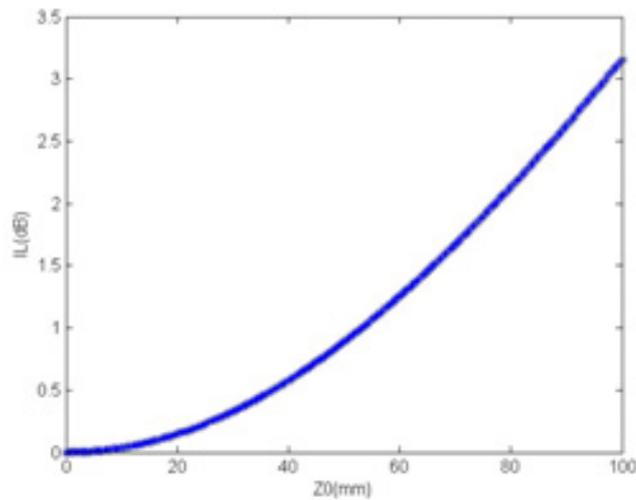Figure 2. Equivalent Sketch of the Single-Optical Fiber Collimator

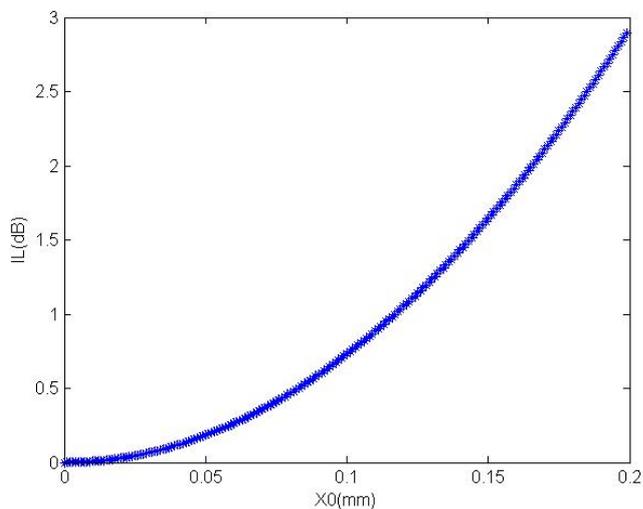Figure 3. $IL \sim Z_0$ Relational Graph: Axial Mismatch $X_0 = 0$, $\theta = 0$

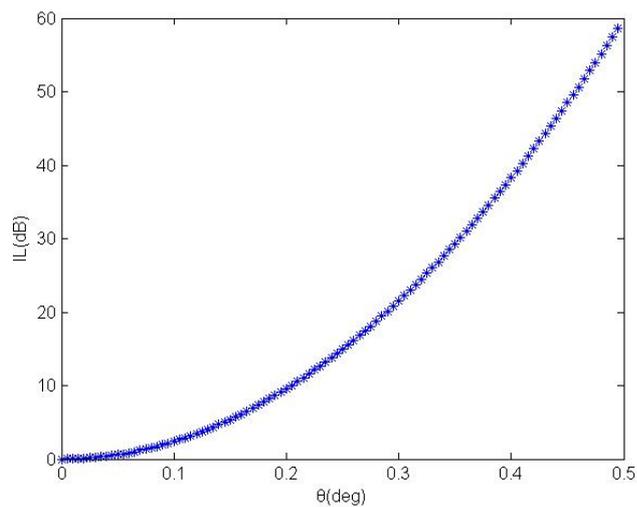Figure 4. $IL \sim X_0$ Relational Graph: Radial Mismatch $Z_0 = 0$, $\theta = 0$

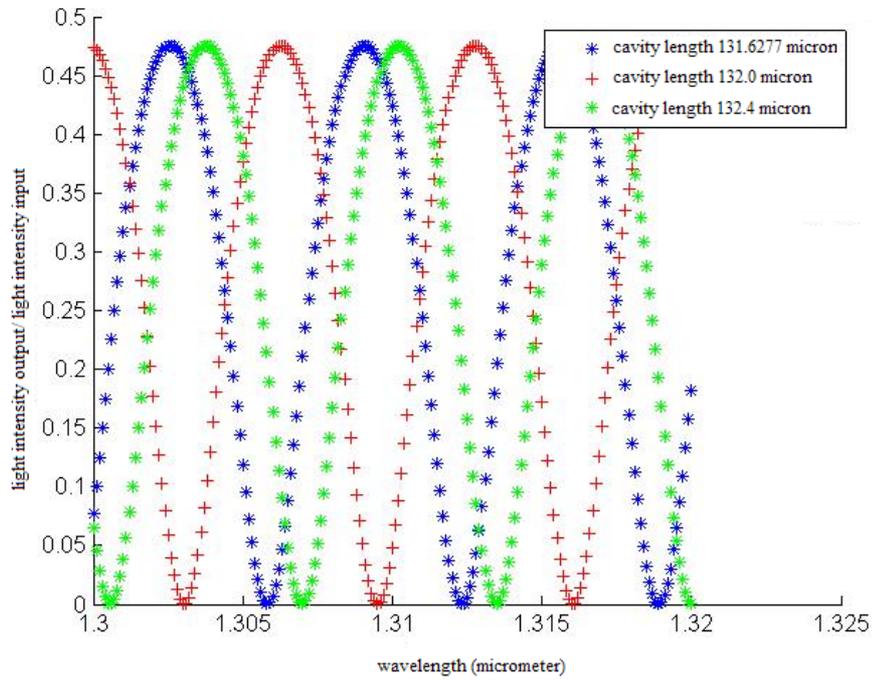Figure 5. $IL \sim \theta$ Relational Graph: Angled Mismatch $X_0 = 0$, $Z_0 = 0$

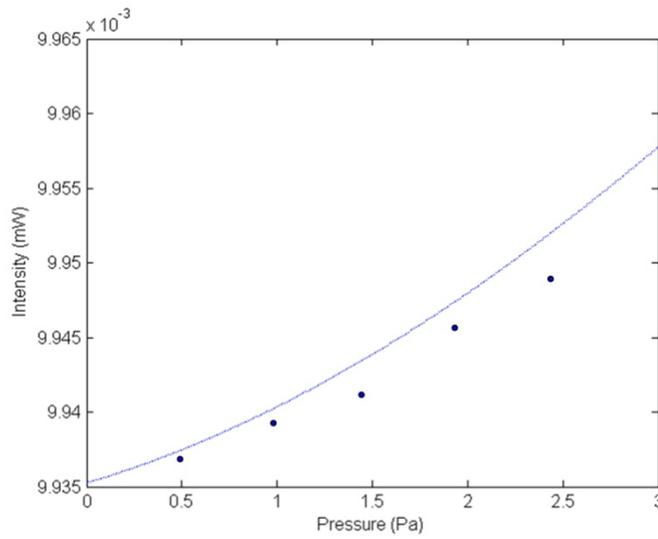Figure 6. Simulation of the Reflection Spectrums for Different Cavity Lengths

Figure 7. Comparison of the Static Pressure Test Result and the Simulation Result